

## Supplemental Information

### Azacrown-Calixpyrrole Isostere: Receptor and Sensor for Anions

Austin R. Sartori, Aco Radujević, Sandra M. George, Pavel Anzenbacher Jr\*.

#### Table of Contents

General Experimental.....	1
Experimental Methods and Characterization Data.....	2
Optical Characterization Data.....	7
<sup>1</sup> H NMR Titration Experiments.....	8
UV-Vis Titration Experiments.....	9
Fluorescence Titration Experiments.....	10
Limit of Detection Determination.....	16
High-throughput (HT) Fluorescence Measurements.....	17
Molecular Modeling.....	23
References.....	30

#### General Experimental

**General:** Commercially available reagents were used as received from the chemical suppliers. Dichloromethane (DCM) was distilled at atm. pressure from CaH<sub>2</sub> and stored under inert atmosphere in the presence of 4Å molecular sieves. Methanol (MeOH) was distilled from magnesium metal and stored under inert atmosphere above 3Å molecular sieves. Reaction progress was monitored using Whatman K6F silica gel 60Å or aluminum analytical thin layer chromatography (TLC) plates by UV detection (254 nm). Column chromatography was performed using silica gel (pore size 60 Å, 230-400 mash), 50-200 µm received from Sorbent Technologies, Inc., Norcross, GA, USA. NMR spectra were recorded using Bruker AVANCE spectrometer operating at 500 MHz for <sup>1</sup>H, and 125 MHz for <sup>13</sup>C NMR. Chemical shifts are given in parts per million from Me<sub>4</sub>Si in CDCl<sub>3</sub>, and DMSO-*d*<sub>6</sub>. The signal multiplicity was described as follows: s (singlet), d (doublet), t (triplet), m (multiplet). Coupling constants (*J*) are reported in hertz (Hz). MALDI (Matrix Assisted Laser Desorption/Ionization) was performed using Shimadzu Biotech AXIMA Performance MALDI TOF/TOF Mass Spectrometer

where dithranol as a matrix. For neutral/positively charged molecules reflectron mode was used.

**UV-vis absorption measurements:** Absorption spectra were acquired using Agilent Cary 60 UV-vis double beam spectrophotometer, absorption spectra and titrations experiments were performed in the range of 250 nm to 500 nm. Parameters: average time 1 ms, 1 nm interval. All solutions were prepared and acquired in standard 1×1 cm quartz cuvettes (3.50 mL volume). Solution of sensor **3** was prepared in DMSO at concentration of 10 μM. Sodium salts of anions were dissolved in Nano pure water (17.5 MΩcm) and their concentrations were in mM to avoid dilution of the host during the titration experiment. After each addition, absorption spectra were recorded.

**Fluorescence measurements:** Steady-state fluorescence emission measurements were conducted using single photon counting spectrofluorometer manufactured by Edinburgh Analytical Instruments (FL/FS 920). All solutions were prepared and measured in fluorimetric 1×1 cm quartz cuvettes (3.50 mL volume). The excitation wavelength was chosen to be 370 nm, where the absorbance of the sensor is constant. Excitation and emission slits were 0.6 and 2.85 nm, respectively. Correction file supplied from the manufacturer were applied to the data. Fluorescence emission scans were acquired between 400 nm and 700 nm. Emission intensity was scanned during the run in 1 nm steps with a dwell time of 0.50 sec. The resulting titrations isotherms were obtained by plotting the intensity change against the concentration of the guest using <http://supramolecular.org/>.<sup>1</sup> All UV-vis and fluorescence titration experiments were performed at least two times for each of the studied analytes to confirm the reproducibility of the results. The fits were evaluated using three criteria: First, the overall fit was visually evaluated for how well the fitting model fits experimental data. Secondly, binding constants were analyzed with respect to the corresponding fitting errors (lower than 20%). Only the fits that yield random distribution of fit residuals were used. The binding stoichiometry was evaluated using Job plot method as well as by the fit quality for 2:1, 1:1 and 1:2 models using the criteria above.

## Experimental Methods and Characterization Data

**Synthesis of sensor 3:** The synthesis was performed in two steps: The first step was the formation of imine products, followed by the reduction of the imine to obtain amine **3**.

All glassware used in this reaction setup was flame dried and cooled down to room temperature in the desiccator. A triple-necked round bottom flask (100 mL), equipped with a dropping funnel, Claisen adapter, and magnetic stir bar, was connected to a dual-manifold Schlenk line. Evacuation/backfilling with dry argon was performed three times, after which the constant positive pressure of dry argon was maintained throughout the reaction. The flask was charged with diamine **6** (66.8 mg, 0.198 mmol) dissolved in dry MeOH (22 mL, freshly

distilled) followed by dropwise addition of dipyrromethane aldehyde **5** (47.3 mg, 0.205 mmol) dissolved in dry MeOH (22 mL). Dropwise addition was controlled for 1 hour using a syringe pump. The reaction mixture was left to stir at room temperature for 72 hours. Then the mixture was concentrated to 1/3 on a rotary evaporator (bath temperature set to 25-30 °C). Undissolved oligomers were filtered off, and the filtrate was overlaid with dry Ar, closed, and left in the freezer overnight for precipitation to occur. The precipitate was filtered off using a Hirsch funnel and collected to obtain 18.7 mg of a yellowish powder. MALDI analysis revealed the presence of acyclic and macrocyclic products dominated by the 2+2 imine compound **7**.

The imine mixture was placed in a small round bottom flask previously flame-dried and cooled in the desiccator. The flask was equipped with a magnetic stir bar and dual flow (vacuum/nitrogen) adapter connected to a Schlenk line. The flask was charged with the imine mixture obtained as described above (18.7 mg). Dry MeOH (2 mL) and dry freshly distilled DCM (1 mL) were added to dissolve the starting material. NaBH<sub>4</sub> (2.5 mg, 0.06 mmol) was added in 3 portions over the course of 45 minutes, and the mixture was stirred for an additional 4 hours at room temperature. Then, the solvents were evaporated using a rotary evaporator (bath temperature was set to 30 °C), and the solid residue was treated by DCM (20 ml). The mixture was filtered through a fritted funnel to remove white solids, and the DCM filtrate was washed with water (3 × 5ml) and dried over anhydrous MgSO<sub>4</sub>. DCM was removed using a rotary evaporator, and the resulting crude mixture was dissolved in the smallest amount of freshly distilled CHCl<sub>3</sub> and layered with hexane until clouding was observed to initiate crystallization/precipitation. The yellow powder precipitate was collected and further purified using column chromatography (SiO<sub>2</sub>, gradient elution; DCM:MeOH:NH<sub>4</sub>OH = 99:1:0.1 → 80:20:3) to yield a yellow crystalline solid (4.35 mg, 23%). TLC was performed using DCM:MeOH:NH<sub>4</sub>OH (80:20:3) using fluorescence detection.

**<sup>1</sup>H NMR (CDCl<sub>3</sub>, 500 MHz)** δ = 1.52 (s, 6H), 2.56 (bt, 4H), 2.86 (s, 6H), 3.17 (bt, 4H), 3.38 (bt, 4H), 5.78 (d, *J* = 27 Hz, 4H), 7.14-7.20 (m, 1H), 7.44-7.46 (m, 2H), 8.09 (d, *J* = 6.5 Hz, 1H), 8.22 (d, *J* = 8.5 Hz, 1H), 8.47-8.53 (m, 1H), 8.77 (bs, 2H) ppm.

**<sup>13</sup>C NMR (CDCl<sub>3</sub>, 125 MHz)** δ = 29.26, 35.46, 45.54, 45.78, 46.74, 47.61, 103.28, 106.35, 115.38, 119.30, 123.36, 128.37, 129.24, 129.60, 130.20, 130.24, 130.60, 134.69, 139.45, 151.97 ppm.

**MS (MALDI-TOF):** 534.6683 *m/z* [M]<sup>+</sup> calcd. for C<sub>29</sub>H<sub>38</sub>N<sub>6</sub>O<sub>2</sub>S 534.2777. Base peak: 533.6632 *m/z* [M-1].

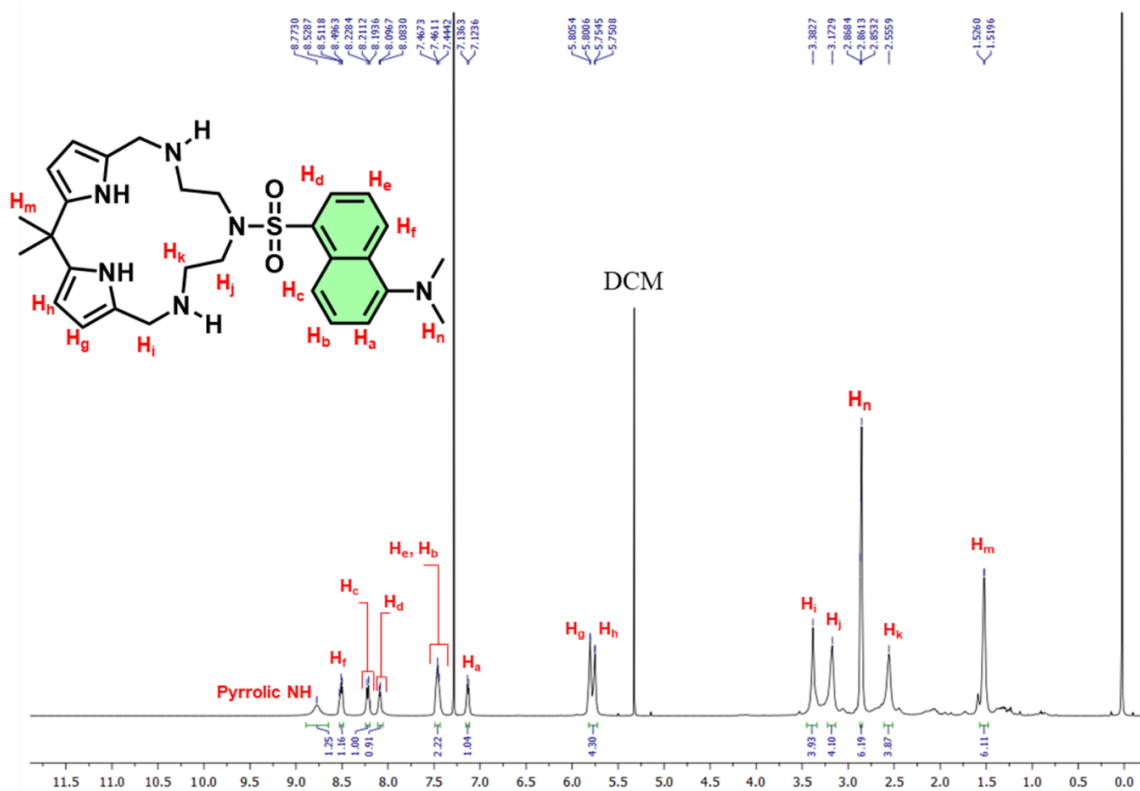


Figure S1.  $^1\text{H}$  NMR (500 MHz,  $\text{CDCl}_3$ ) spectrum of an amine macrocycle **3**.

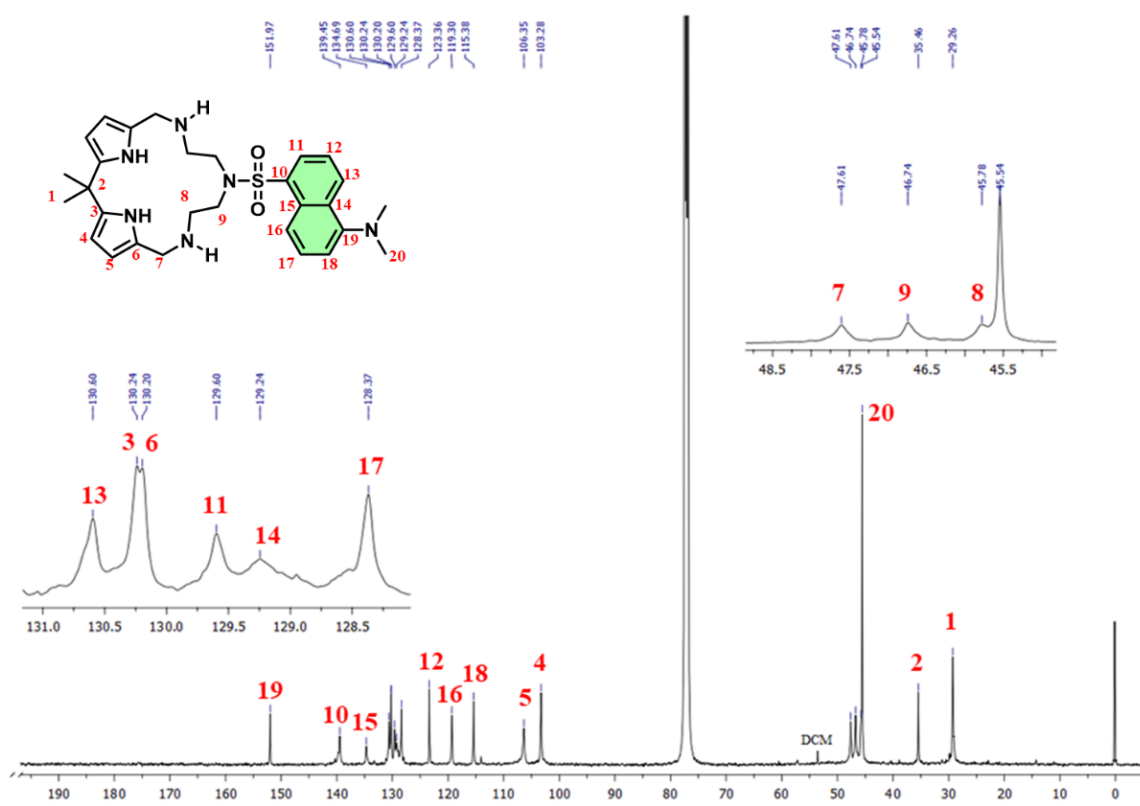
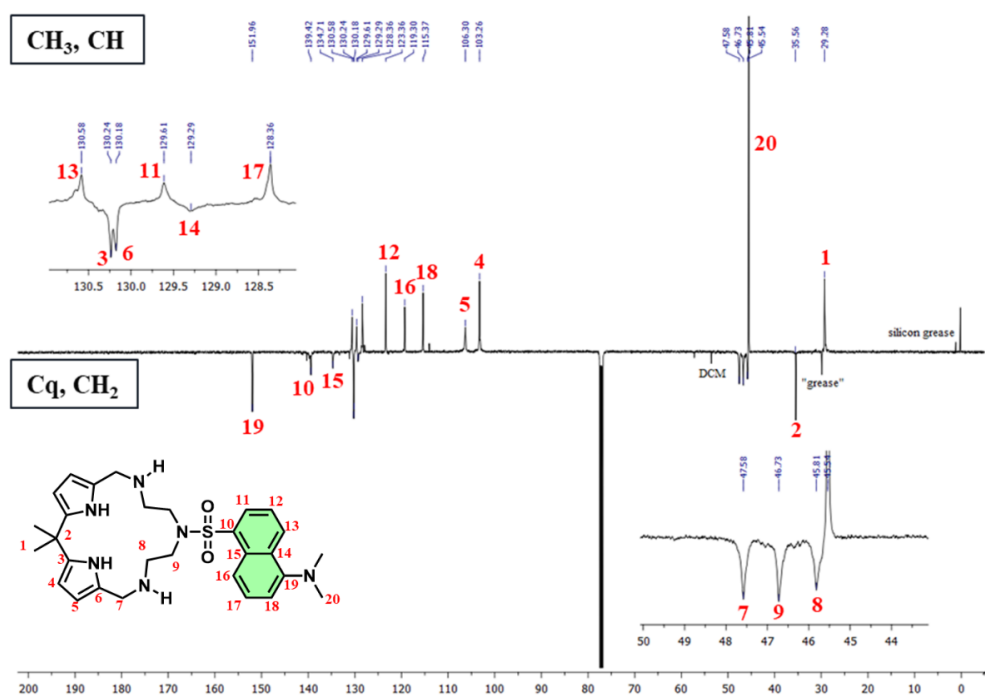
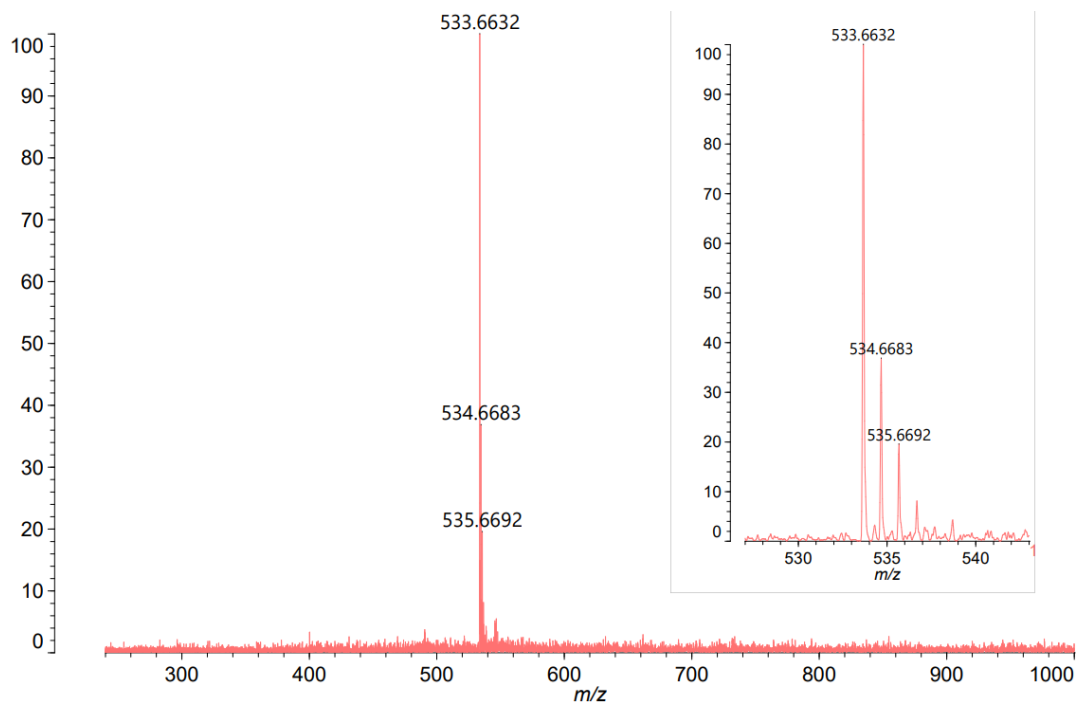


Figure S2.  $^{13}\text{C}$  NMR (125 MHz,  $\text{CDCl}_3$ ) of amine macrocycle **3**.



**Figure S3.** <sup>13</sup>C APT-NMR (125 MHz, CDCl<sub>3</sub>) of amine macrocycle **3**. The quaternary and methylene carbons are phased negative, methine and methyl carbons are phased positive.



**Figure S4.** MALDI-TOF spectrum of sensor **3** (positive mode, dithranol matrix).

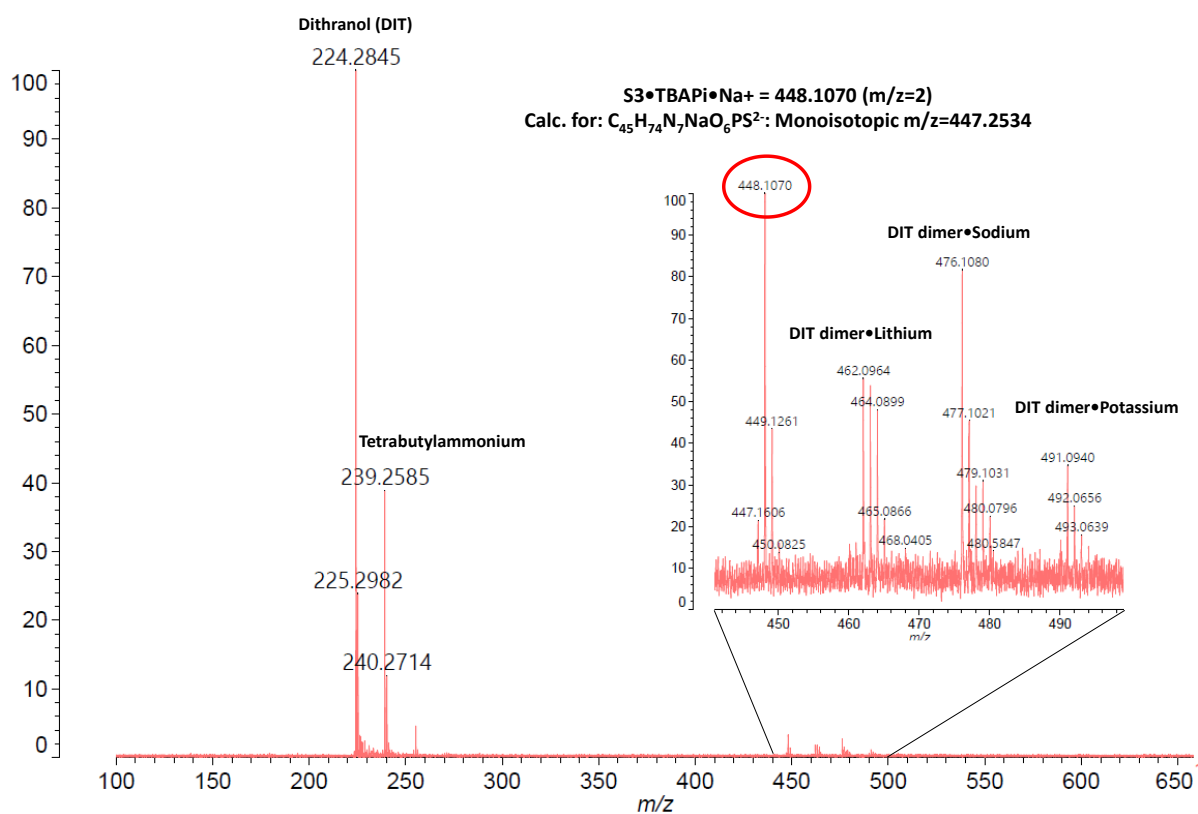


**Figure S5.** Low-resolution MALDI-TOF spectrum of sensor **3**•Tetrabutylammoniumphosphate (TBAPi) •Sodium (negative mode, dithranol matrix).

## Optical Characterization Data

**Fluorescence lifetime measurement:** The fluorescence lifetime ( $\tau_f$ ) measurement of **3** ( $1 \times 10^{-5}$  M in DMSO:water (85:15 v:v)) was recorded using an FLS1000 photoluminescence spectrometer in conjunction with a EPL -375 picosecond pulsed diode laser and was determined to be: 12.5 ns. ( $\lambda_{exc} = 375$  nm)

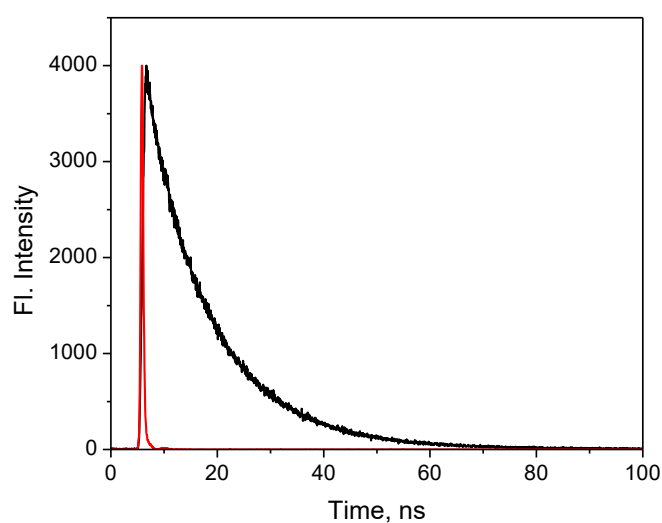


**Figure S6.** Fluorescence lifetime of **3** ( $1 \times 10^{-5}$  M in DMSO:water (85:15 v:v)) (black line) and the instrument response function (red line).  $\lambda_{exc} = 375$  nm.

**Quantum yield:** The quantum yield of **3**, dissolved in 15% water in DMSO, was recorded using Hamamatsu absolute quantum yield spectrometer Quantaurus C11347 and was determined to be: 49%. ( $\lambda_{exc} = 350$  nm)

## $^1\text{H}$ NMR Titration Experiments

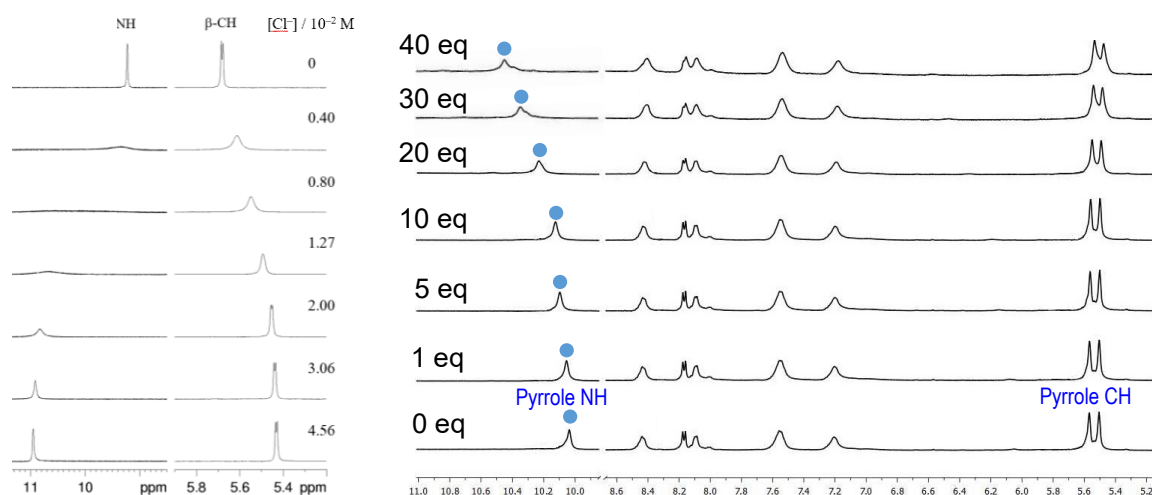


**Figure S7.**  $^1\text{H}$  NMR (500 MHz,  $\text{DMSO-}d_6$ ) titration of receptors with TBACl. **Left panel:** Octamethyl-calix[4]pyrrole (CP,  $1 \times 10^{-2}$  M) shows significant shifts of pyrrole NH and pyrrole  $\beta$ -CH resonances upon addition of the chloride salt. **Right panel:** Titration of sensor **3** ( $8.31 \times 10^{-3}$  M) with chloride did not result in significant shifts up to 10+ equivalents of chloride.

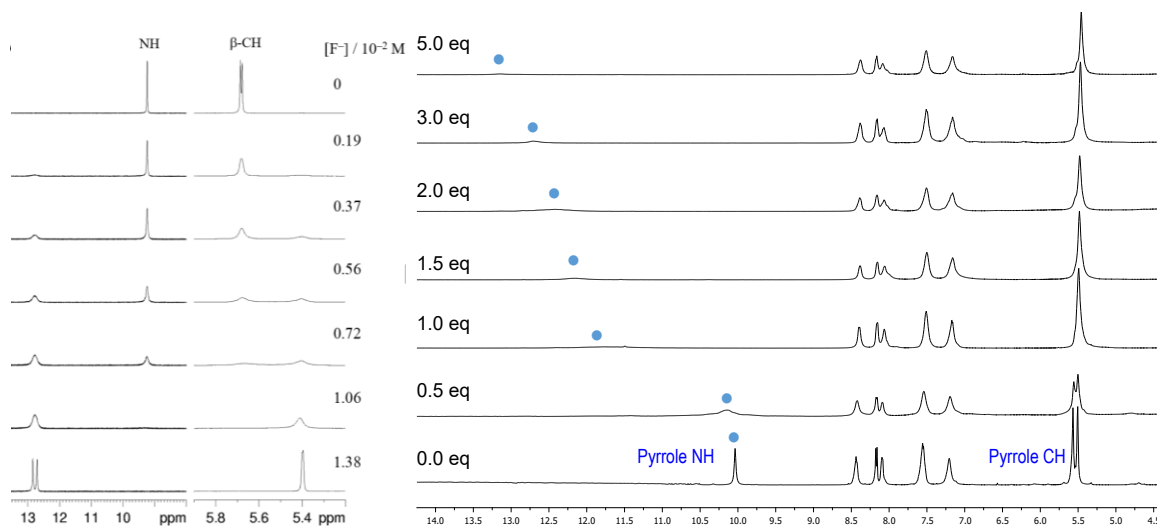


**Figure S8.**  $^1\text{H}$  NMR (500 MHz,  $\text{DMSO-}d_6$ ) titration of receptors with TBAF. **Left panel:** Octamethyl-calix[4]pyrrole (CP,  $1 \times 10^{-2}$  M) shows significant shifts of pyrrole NH and pyrrole  $\beta$ -CH resonances upon addition of the fluoride salt. **Right panel:** Titration of sensor **3** ( $8.31 \times 10^{-3}$  M) results in a disappearance of the NH resonances due to deprotonation while the pyrrole  $\beta$ -CH resonances show only a small shift.

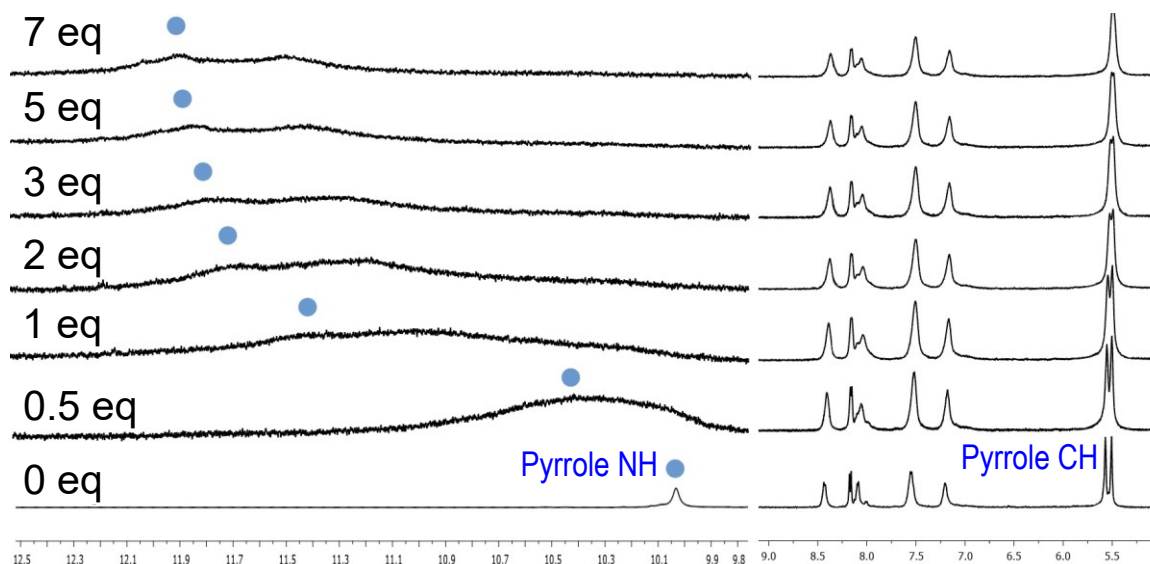


**Figure S9.**  $^1\text{H}$  NMR (500 MHz,  $\text{DMSO-}d_6$ ) titration of sensor **3** ( $8.31 \times 10^{-3}$  M) with  $\text{TBAH}_2\text{PO}_4$  shows a significant shift in pyrrole NH resonances suggesting a strong sensor-phosphate binding.

## UV-Vis Titration Experiments

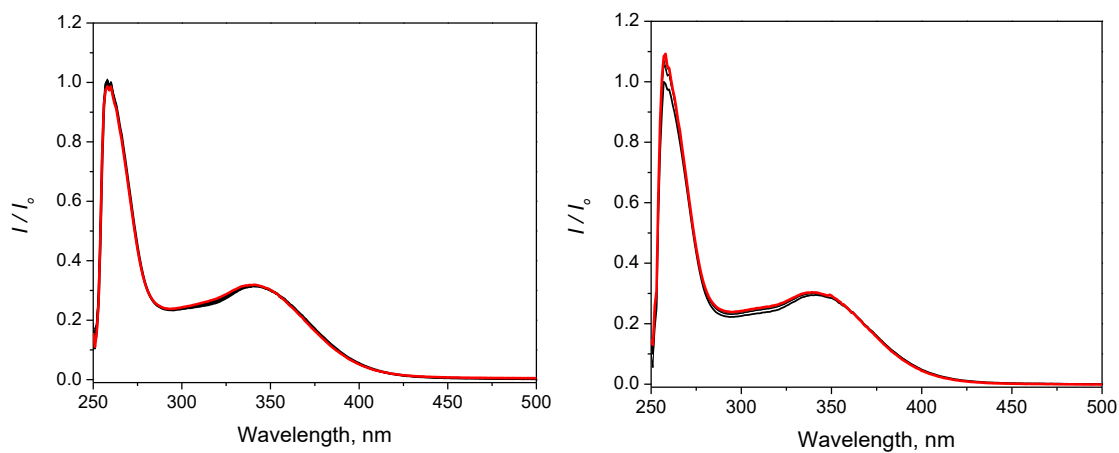


**Figure S10.** Absorption spectra of the sensor **3** ( $9 \times 10^{-5}$  M in  $\text{DMSO}:\text{water}$  (85:15 v:v)) **Left:** upon addition of  $\text{NaH}_2\text{PO}_4$ ; **Right:** pyrophosphate in water.

## Fluorescence Titration Experiments

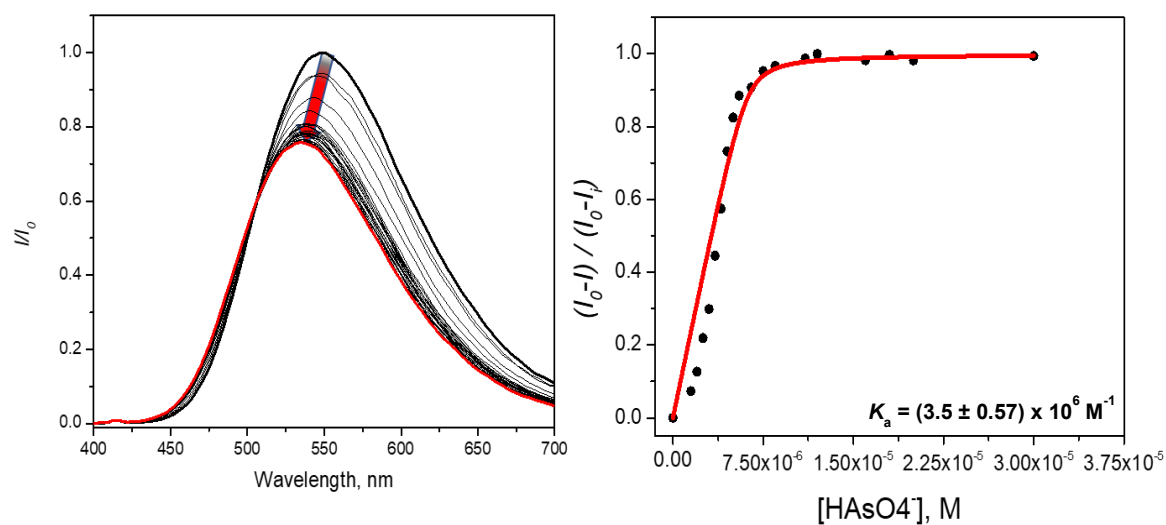


**Figure S11.** Fluorescence spectra and isotherm of **3** ( $1 \times 10^{-5} \text{ M}$  in DMSO:water (85:15 v:v)) upon incremental addition of  $\text{Na}_2\text{HAsO}_4$  in water.  $\lambda_{\text{exc}} = 370 \text{ nm}$ .

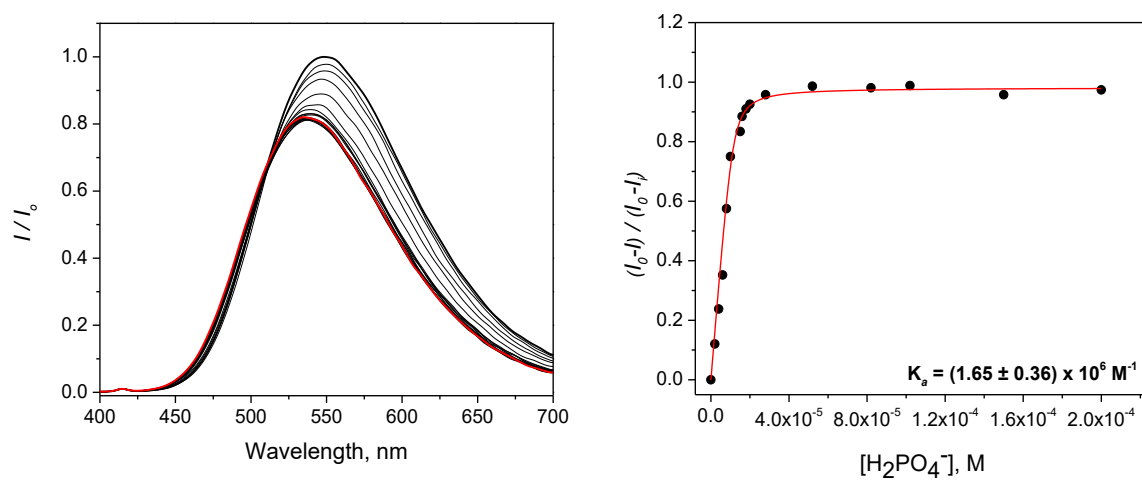


**Figure S12.** Fluorescence spectra and isotherm of **3** ( $1 \times 10^{-5} \text{ M}$  in DMSO:water (85:15 v:v)) upon incremental addition of  $\text{NaH}_2\text{PO}_4$  in water.  $\lambda_{\text{exc}} = 370 \text{ nm}$ .

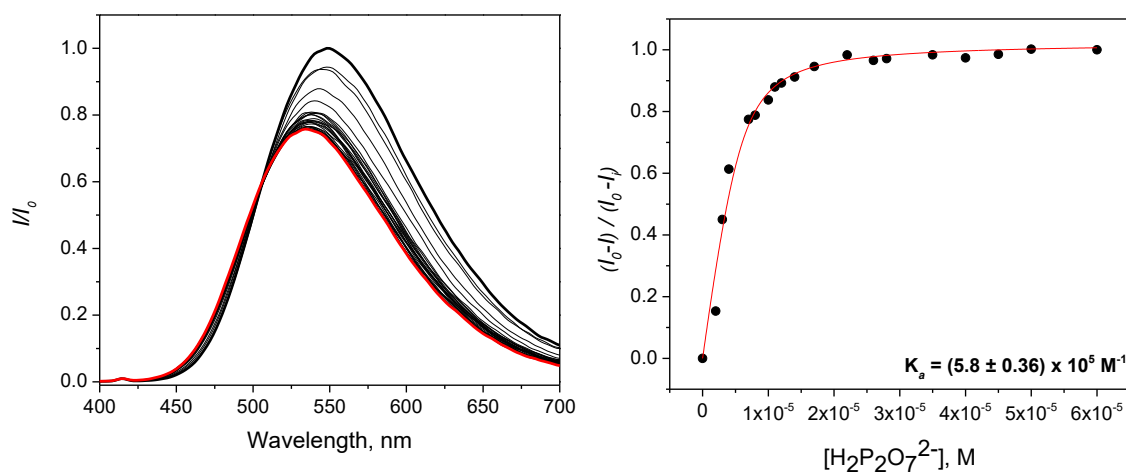


**Figure S13.** Fluorescence spectra and isotherm of **3** ( $1 \times 10^{-5}$  M in DMSO:water (85:15 v:v)) upon incremental addition of  $\text{Na}_2\text{H}_2\text{P}_2\text{O}_7$  in water.  $\lambda_{\text{exc}} = 370$  nm.

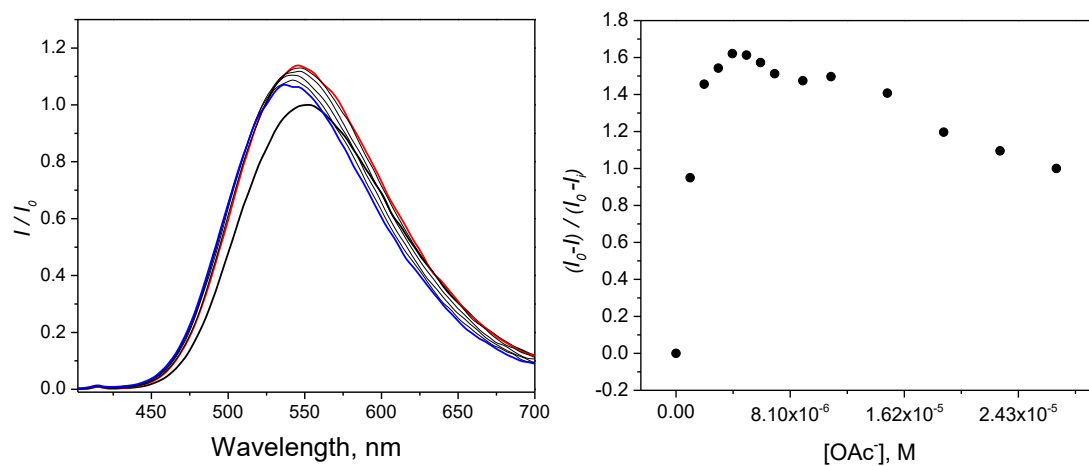


**Figure S14.** Fluorescence spectra and isotherm of **3** ( $1 \times 10^{-5}$  M in DMSO:water (85:15 v:v)) upon incremental addition of TBAOAc in water.  $\lambda_{\text{exc}} = 370$  nm.

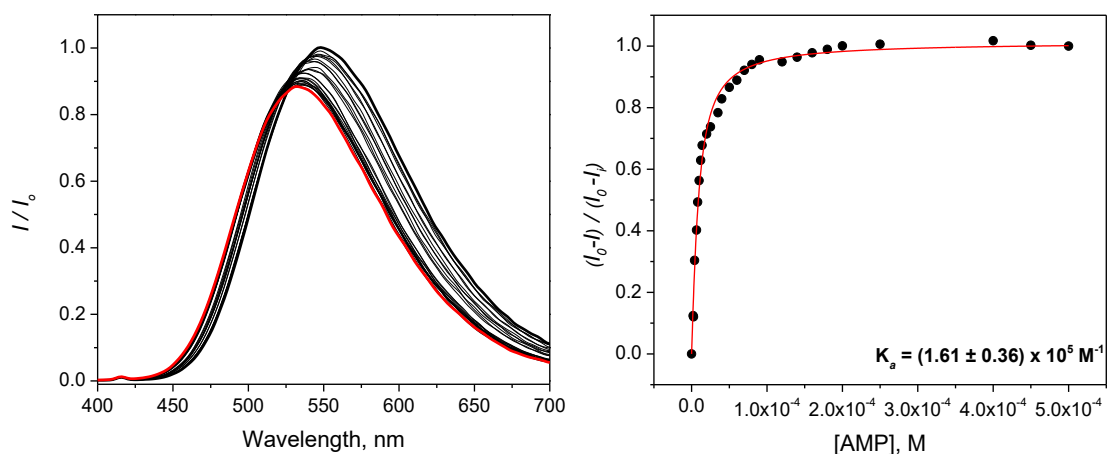


**Figure S15.** Fluorescence spectra and isotherm of **3** ( $1 \times 10^{-5}$  M in DMSO:water (85:15 v:v)) upon incremental addition of NaAMP in water.  $\lambda_{\text{exc}} = 370$  nm.

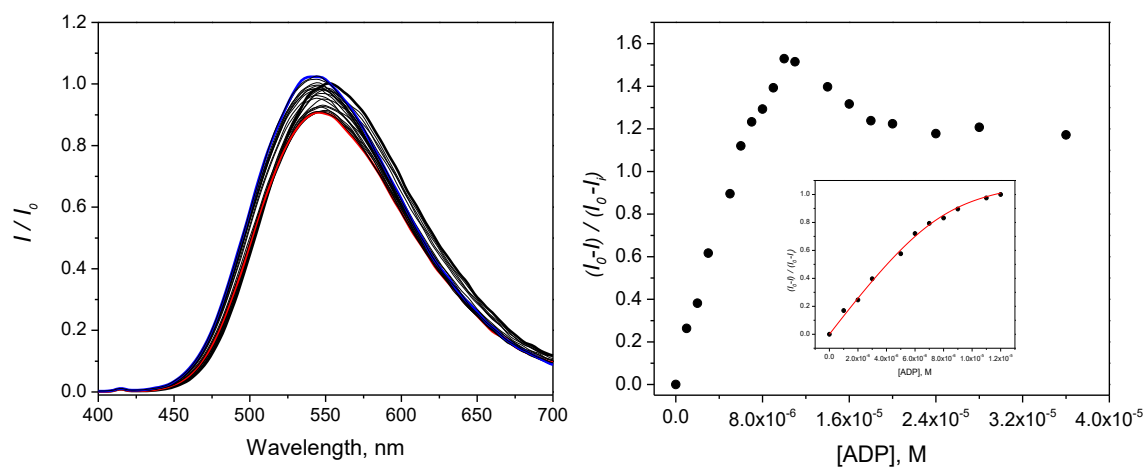


**Figure S16.** Fluorescence spectra and isotherm of amine macrocycle **3** ( $1 \times 10^{-5}$  M in DMSO:water (85:15 v:v)) upon incremental addition of  $\text{Na}_2\text{ADP}$  in water.  $\lambda_{\text{exc}} = 370$  nm.

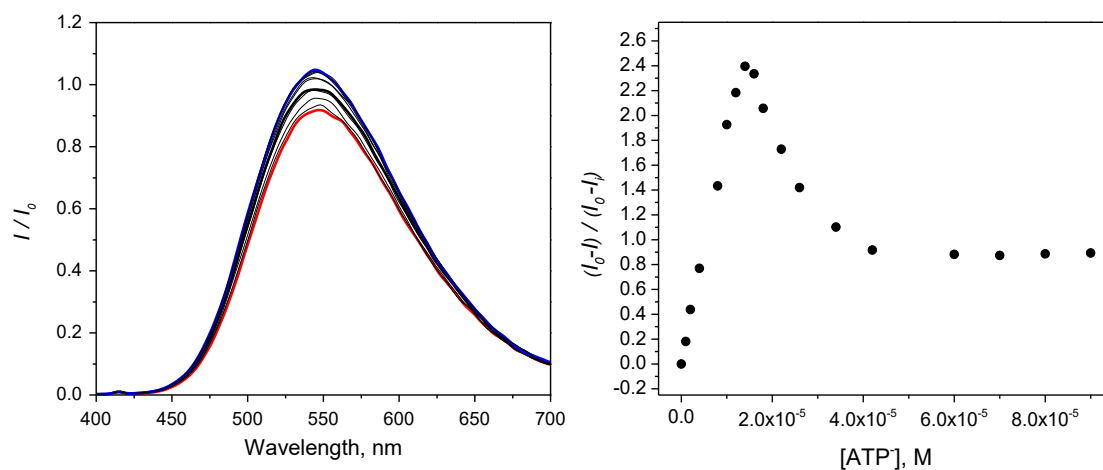


**Figure S17.** Fluorescence spectra and isotherm of **3** ( $1 \times 10^{-5}$  M in DMSO:water (85:15 v:v)) upon incremental addition of  $\text{Na}_2\text{ATP}$  in water.  $\lambda_{\text{exc}} = 370$  nm.

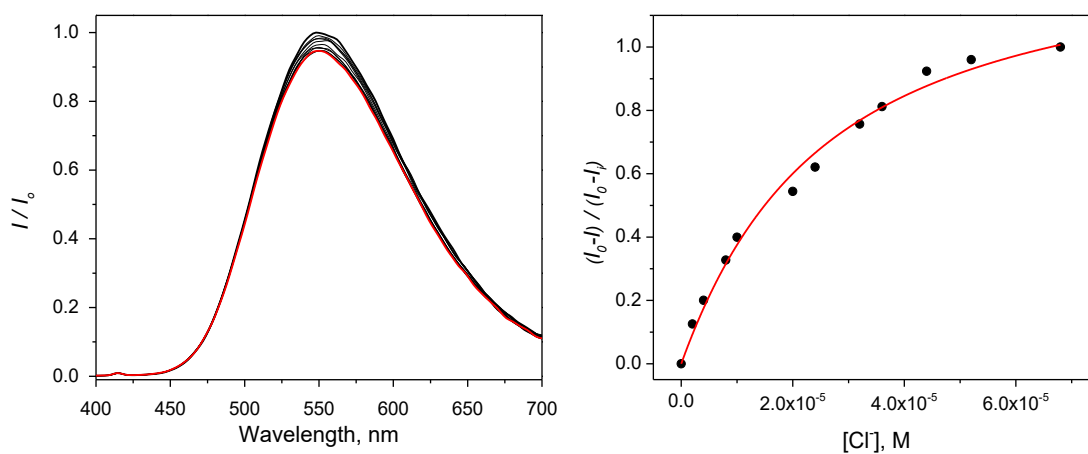


**Figure S18.** Fluorescence spectra and isotherm of **3** ( $1 \times 10^{-5}$  M in DMSO:water (85:15 v:v)) upon incremental addition of  $\text{NaCl}$  in water.  $\lambda_{\text{exc}} = 370$  nm.

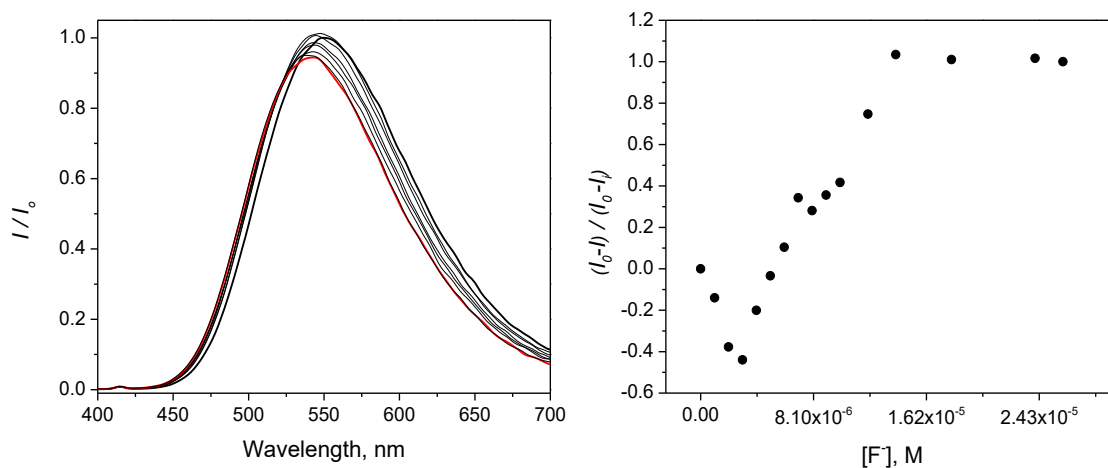


**Figure S19.** Fluorescence spectra and isotherm of **3** ( $1 \times 10^{-5}$  M in DMSO:water (85:15 v:v)) upon incremental addition of TBAF in water.  $\lambda_{\text{exc}} = 370$  nm.

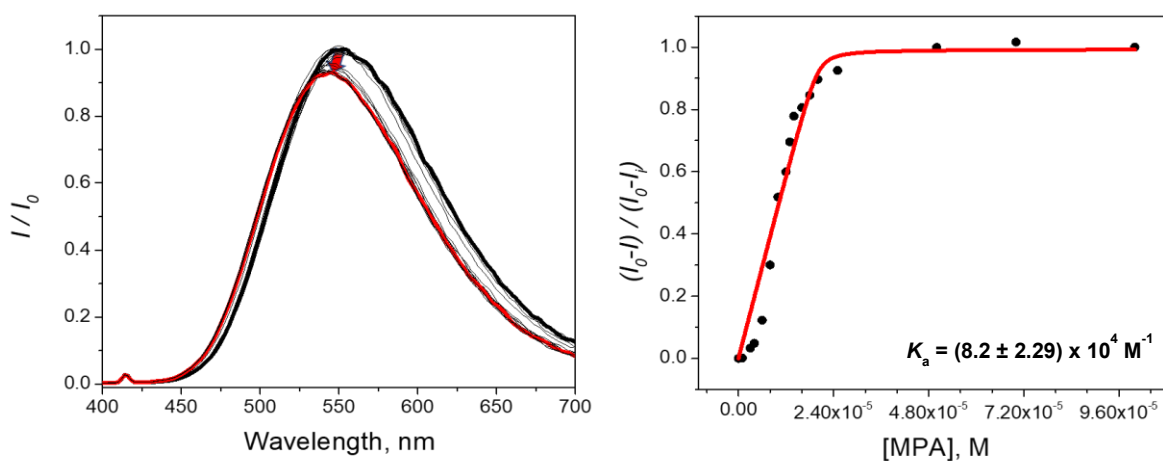


**Figure S20.** Fluorescence spectra and isotherm of **3** ( $1 \times 10^{-5}$  M in DMSO:water (85:15 v:v)) upon incremental addition of NaMPA in water.  $\lambda_{\text{exc}} = 370$  nm.

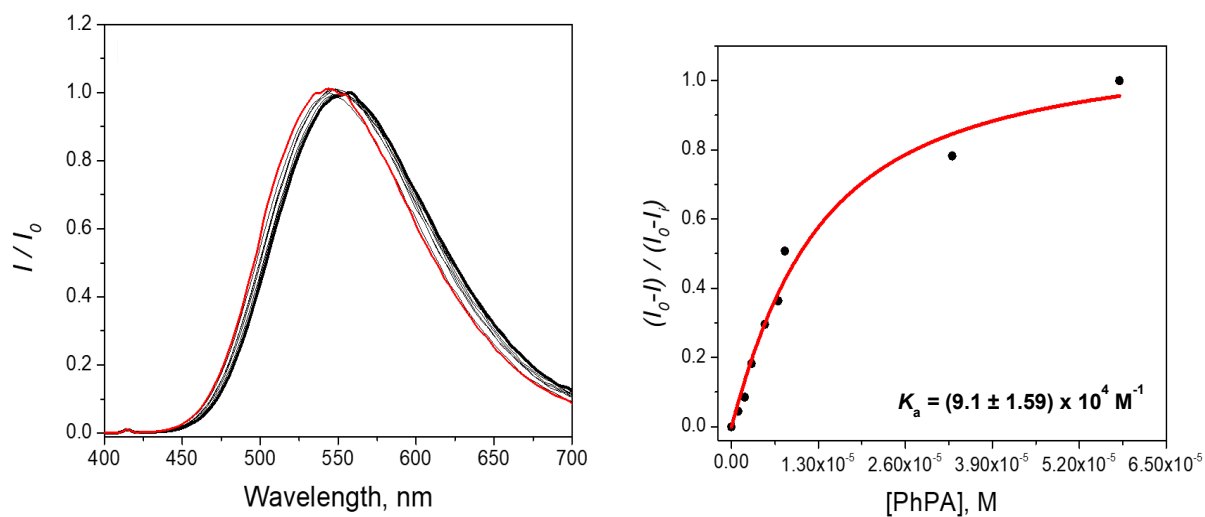


**Figure S21.** Fluorescence spectra and isotherm of **3** (1 × 10<sup>-5</sup> M in DMSO:water (85:15 v:v)) upon incremental addition of NaPhPA in water.  $\lambda_{\text{exc}} = 370 \text{ nm}$ .

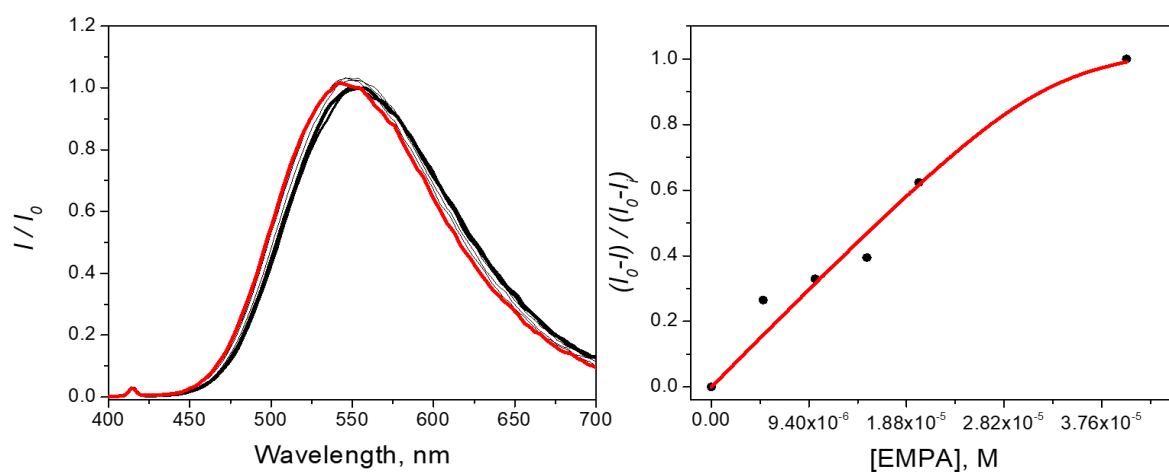


**Figure S22.** Fluorescence spectra and isotherm of **3** (1 × 10<sup>-5</sup> M in DMSO:water (85:15 v:v)) upon incremental addition of NaEMPA in water.  $\lambda_{\text{exc}} = 370 \text{ nm}$ .

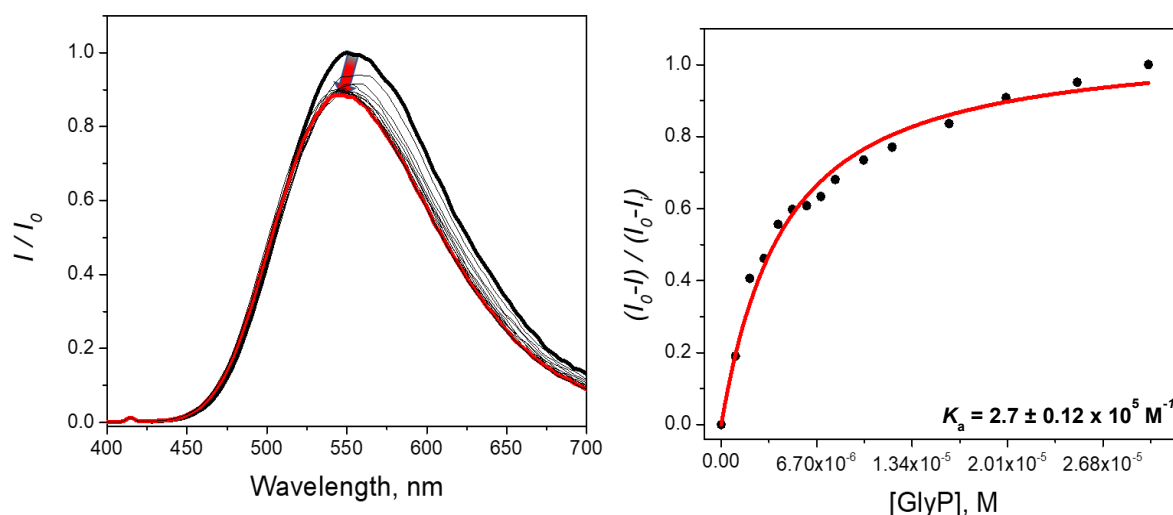


**Figure S23.** Fluorescence spectra and isotherm of **3** ( $1 \times 10^{-5}$  M in DMSO:water (85:15 v:v)) upon incremental addition of  $\text{Na}_2\text{GlyP}$  in water.  $\lambda_{\text{exc}} = 370$  nm.

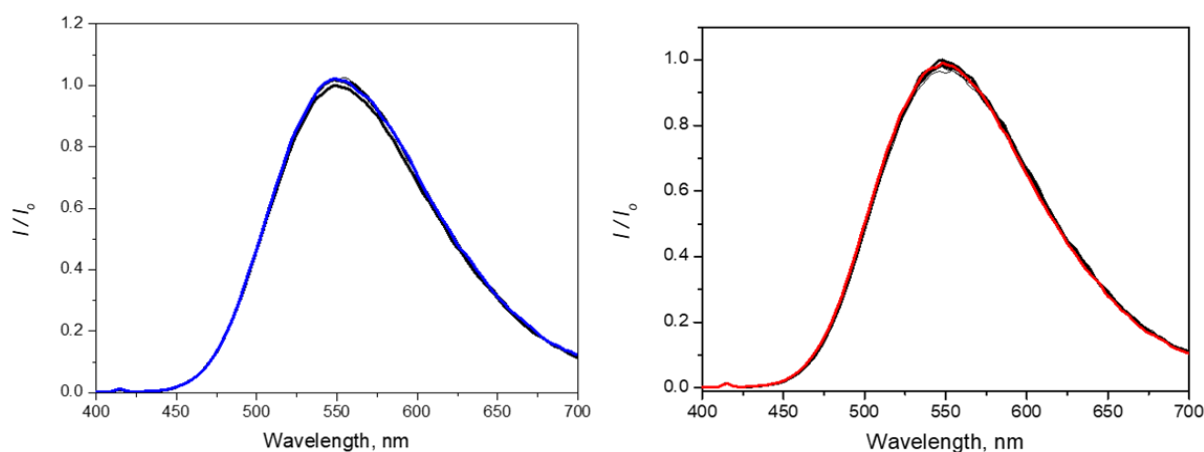


**Figure S24.** Fluorescence titration spectra of **3** ( $1 \times 10^{-5}$  M in DMSO:water (85:15 v:v)) upon addition of: **Left:**  $\text{NaNO}_3$ ; **Right:**  $\text{NaHSO}_4$  in water.  $\lambda_{\text{exc}} = 370$  nm.

### Limit of Detection Determination

The detection limit (LOD) was determined from a linear regression analysis of the fluorescence titration data versus the concentration for each analyte ( $\text{LOD} = (3.3\sigma/m)$ ). The LOD was determined to be  $0.6 \mu\text{M}$ ,  $0.7 \mu\text{M}$ , and  $1 \mu\text{M}$  for orthophosphate, glyphosate, and methylphosphonate, respectively.

## High-throughput (HT) Fluorescence Measurements

**Determination of analyte-specific spectral response via linear discriminant analysis:** The emission spectra were acquired using a fluorescence spectrometer ( $\lambda_{\text{exc}} = 370 \text{ nm}$ ), 20 replicas of each of the ten analytes (the nine phosphates/phosphonates and water as a control) at a 1:3 mixture of sensor **3** to analyte. The observed changes in the fluorescence intensities (at the maximum), full width at half maximums (FWHM), and the hypsochromic shifts (Table 1) were evaluated to determine whether these provide an analyte-specific response to enable a reliable and unambiguous classification of the analytes. Therefore, parameters were subjected to linear discriminant analysis (LDA), and the resulting LDA clearly shows a successful qualitative analysis of these analytes (Fig. 5A & S25-26).

**Qualitative assay:** A stock solution of the sensor (5.56  $\mu\text{M}$ ) was made in DMSO. Stock solutions of the analytes (Pi, PPi, AMP, ADP, ATP, MPA, PhPA, EMPA, and GlyP) were made in ultra-pure water (150  $\mu\text{M}$ ). Using an 8-channel micropipette, 90  $\mu\text{L}$  of stock solution containing the sensor was dispensed into 384 well microplates (MATRICAL MP100-1-PS, working volume 100  $\mu\text{L}$ ) followed by an addition of 10  $\mu\text{L}$  of the 150  $\mu\text{M}$  stock solutions of the targeted phosphates and phosphonates. The final concentration of Sensor **3** and targeted analytes was 5  $\mu\text{M}$  and 15  $\mu\text{M}$ , respectively. After dispensing the analytes mixtures, a BMG CLARIOstar microplate reader was used to record the fluorescence intensities from each well. Twelve different combinations of excitation and emission channels were used: ex. 275 nm and em. 500 nm, ex. 275 nm and em. 550 nm, ex. 275 nm and em. 630 nm, ex. 320 nm and em. 500, ex. 320 nm and em. 550, ex. 320 nm and em. 630, ex. 350 nm and em. 500, ex. 350 nm and em. 550, ex. 350 nm and em. 630, ex. 375 nm and em. 500, ex. 375 nm and em. 550, ex. 375 nm and em. 630. The resulting FI. data output was subjected to the Student's t-test to exclude outliers, resulting in 20 final repetitions for each cluster. Finally, the acquired data was analyzed using LDA. The resulting LDA clearly shows a successful qualitative analysis of these analytes (Fig. 5B & S27-28).

**Quantitative assay for methylphosphonate and glyphosate:** A stock solution of the sensor (11.11  $\mu\text{M}$ ) in DMSO was prepared. Analytes MPA and GlyP were dissolved in ultra-pure water in the range of 20 - 300  $\mu\text{M}$  stock solutions. Using an 8-channel micropipette, 90  $\mu\text{L}$  stock solution of the sensor was dispensed into 384 well microplates (MATRICAL MP100-1-PS, working volume 100  $\mu\text{L}$ ) followed by addition of 10  $\mu\text{L}$  of various stock solutions of MPA and GlyP in the range of 0 - 600  $\mu\text{M}$ . The final concentration of sensor **3** and targeted analytes was 10  $\mu\text{M}$  (sensor) and 0 - 60  $\mu\text{M}$  (analyte) respectively. After dispensing the proper analytes mixtures, a BMG CLARIOstar microplate reader was used to collect the fluorescence intensities from each well. Twelve different combinations of excitation and emission channels were used: ex. 275 nm and em. 500 nm, ex. 275 nm and em. 550 nm, ex. 275 nm and em. 630

nm, ex. 320 nm and em. 500, ex. 320 nm and em. 550, ex. 320 nm and em. 630, ex. 350 nm and em. 500, ex. 350 nm and em. 550, ex. 350 nm and em. 630, ex. 375 nm and em. 500, ex. 375 nm and em. 550, ex. 375 nm and em. 630. The resulting FI. data output were subjected to the Student's t-test to exclude outliers, resulting in 20 final repetitions for each cluster. Finally, the acquired data was analyzed using LDA and SVM analysis (Fig. 6A-B and S29-30 (GlyP), Fig. 6C-D and S31-32 (MPA)).

**Quantitative assay for glyphosate in the presence of orthophosphate:** A stock solution of the sensor (11.11  $\mu\text{M}$ ) was made in DMSO. The dihydrogen phosphate (Pi) interferent was made in ultra-pure water (120  $\mu\text{M}$ ). The stock solutions of glyphosate (GlyP) analyte were made in ultra-pure water in varying concentrations (40 – 1,200  $\mu\text{M}$ ). Using an 8-channel micropipette, 90  $\mu\text{L}$  of the stock solution of the sensor was dispensed into 384 well microplates (MATRICAL MP100-1-PS, working volume 100  $\mu\text{L}$ ), followed by the addition of 5  $\mu\text{L}$  of the Pi stock solution and 5  $\mu\text{L}$  of various stock solutions of GlyP. The final concentration of Sensor **3** was 10  $\mu\text{M}$ , the concentration of Pi was 6  $\mu\text{M}$ , and the GlyP concentration was varied from 0 - 60  $\mu\text{M}$ . After dispensing the analytes mixtures, a BMG CLARIOstar microplate reader was used to collect the fluorescence intensities from each well. Twelve different combinations of excitation and emission channels were used: ex. 275 nm and em. 500 nm, ex. 275 nm and em. 550 nm, ex. 275 nm and em. 630 nm, ex. 320 nm and em. 500, ex. 320 nm and em. 550, ex. 320 nm and em. 630, ex. 350 nm and em. 500, ex. 350 nm and em. 550, ex. 350 nm and em. 630, ex. 375 nm and em. 500, ex. 375 nm and em. 550, ex. 375 nm and em. 630. The resulting FI. data output were subjected to the Student's t-test to exclude outliers, resulting in 20 final repetitions for each cluster. Finally, the acquired data was analyzed using LDA and SVM analysis (Fig. 7 and S33-34).

Jackknifed Classification Matrix

	ADP-15uM	AMP-15uM	ATP-15uM	EMPA-15uM	Gly-15uM	MPA-15uM	PhPA-15uM	Pi-15uM	Ppi-15uM	ctrl	%correct
ADP-15uM	20	0	0	0	0	0	0	0	0	0	100
AMP-15uM	0	20	0	0	0	0	0	0	0	0	100
ATP-15uM	0	0	20	0	0	0	0	0	0	0	100
EMPA-15uM	0	0	0	20	0	0	0	0	0	0	100
Gly-15uM	0	0	0	0	20	0	0	0	0	0	100
MPA-15uM	0	0	0	0	0	20	0	0	0	0	100
PhPA-15uM	0	0	0	0	0	0	20	0	0	0	100
Pi-15uM	0	0	0	0	0	0	0	20	0	0	100
Ppi-15uM	0	0	0	0	0	0	0	0	20	0	100
ctrl	0	0	0	0	0	0	0	0	0	20	100
Total	20	20	20	20	20	20	20	20	20	20	100

**Figure S25.** Jackknifed Classification Matrix for LDA constructed with the data recorded using a fluorescence spectrometer (% of quenching, FWHM and wavelength shifts) as an input.

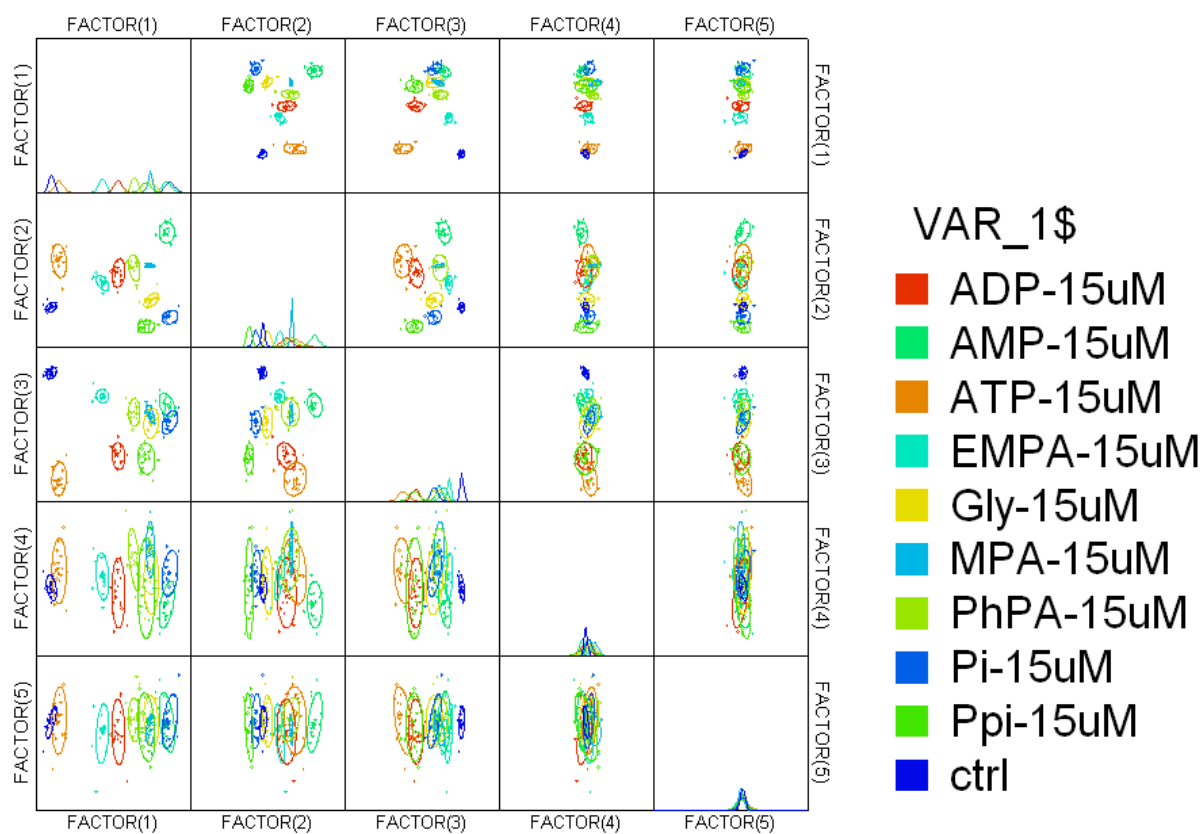


**Figure S26.** LDA canonical scores plot for the data recorded using a fluorescence spectrometer (% of quenching, FWHM and wavelength shifts) as an input.

Jackknifed Classification Matrix

	ADP-20uM	AMP-20uM	ATP-20uM	Ctrl	EMPA-20uM	Gly-20uM	MPA-20uM	PhPA-20uM	Pi-20uM	Ppi-20uM	%correct
ADP-20uM	20	0	0	0	0	0	0	0	0	0	100
AMP-20uM	0	20	0	0	0	0	0	0	0	0	100
ATP-20uM	0	0	20	0	0	0	0	0	0	0	100
Ctrl	0	0	0	20	0	0	0	0	0	0	100
EMPA-20uM	0	0	0	0	20	0	0	0	0	0	100
Gly-20uM	0	0	0	0	0	20	0	0	0	0	100
MPA-20uM	0	0	0	0	0	0	20	0	0	0	100
PhPA-20uM	0	0	0	0	0	0	0	20	0	0	100
Pi-20uM	0	0	0	0	0	0	0	0	20	0	100
Ppi-20uM	0	0	0	0	0	0	0	0	0	20	100
Total	20	20	20	20	20	20	20	20	20	20	100

Figure S27. Jackknifed Classification Matrix for LDA of qualitative assay for sensor 3 and its complexes with phosphates and phosphonates.

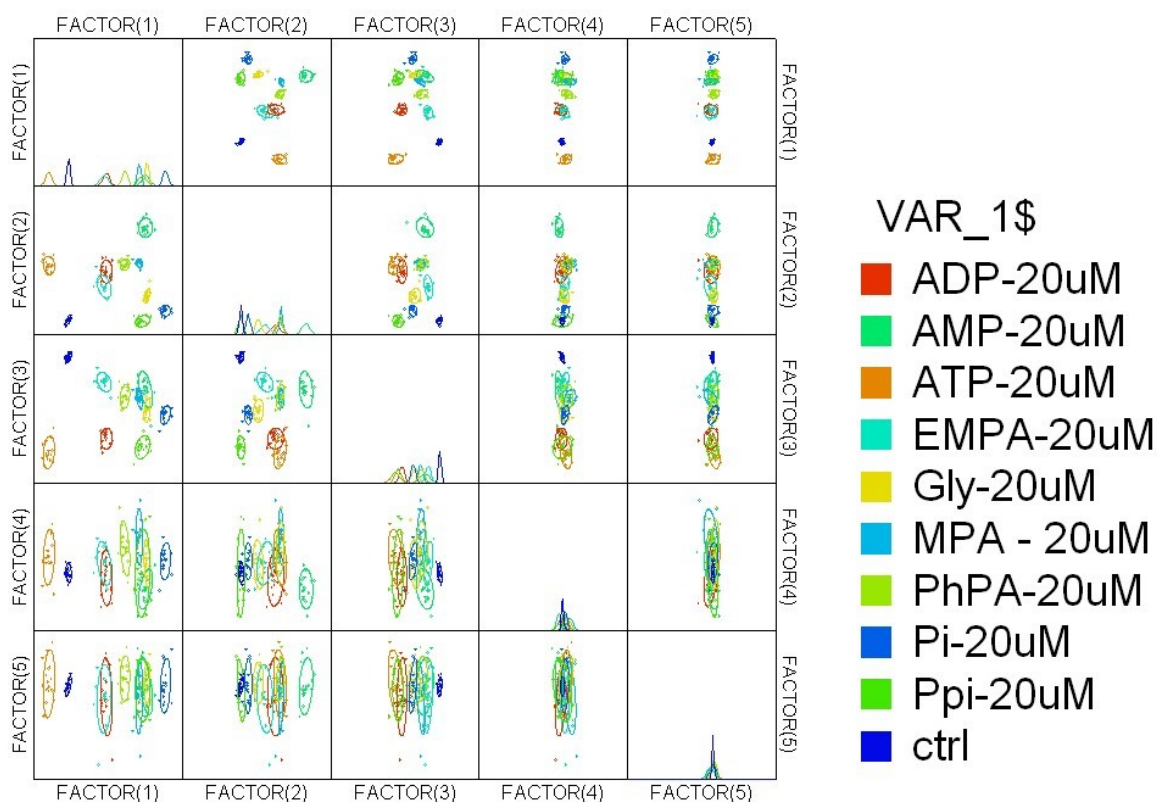
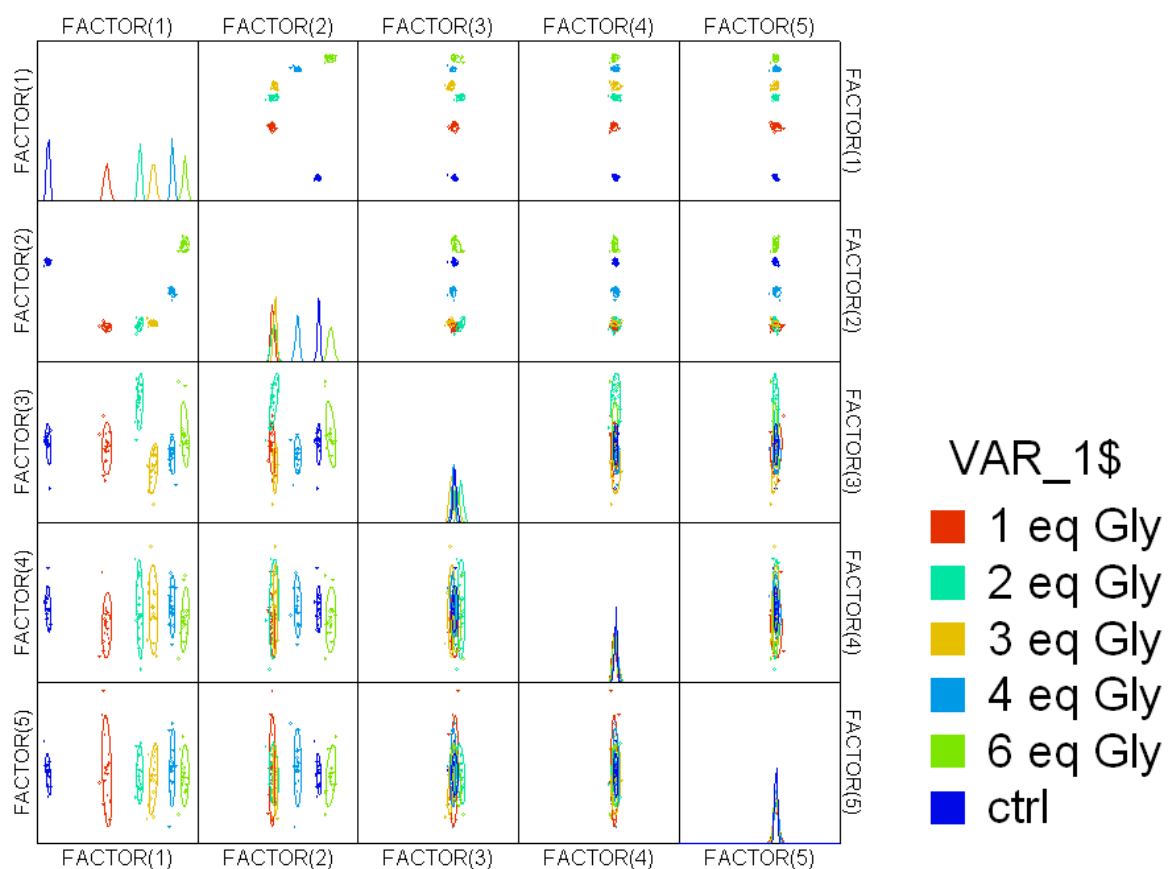


Figure S28. LDA canonical scores plot for the qualitative assay using sensor 3 and its complexes with phosphates and phosphonates.

### Jackknifed Classification Matrix

	1 eq Gly	2 eq Gly	3 eq Gly	4 eq Gly	6 eq Gly	ctrl	%correct
1 eq Gly	20	0	0	0	0	0	100
2 eq Gly	0	20	0	0	0	0	100
3 eq Gly	0	0	20	0	0	0	100
4 eq Gly	0	0	0	20	0	0	100
6 eq Gly	0	0	0	0	20	0	100
ctrl	0	0	0	0	0	20	100
Total	20	20	20	20	20	20	100

**Figure S29.** Jackknifed Classification Matrix of the quantitative LDA assay for sensor 3 and GlyP.



**Figure S30.** LDA canonical scores plot of the quantitative assay for sensor 3 and GlyP.

**Jackknifed Classification Matrix**

	0.5 eq MPA	1 eq MPA	2 eq MPA	3 eq MPA	5 eq MPA	ctrl	%correct
0.5 eq MPA	20	0	0	0	0	0	100
1 eq MPA	0	20	0	0	0	0	100
2 eq MPA	0	0	20	0	0	0	100
3 eq MPA	0	0	0	20	0	0	100
5 eq MPA	0	0	0	0	20	0	100
ctrl	0	0	0	0	0	20	100
Total	20	20	20	20	20	20	100

**Figure S31.** Jackknifed Classification Matrix of the quantitative LDA assay for sensor **3** and MPA.

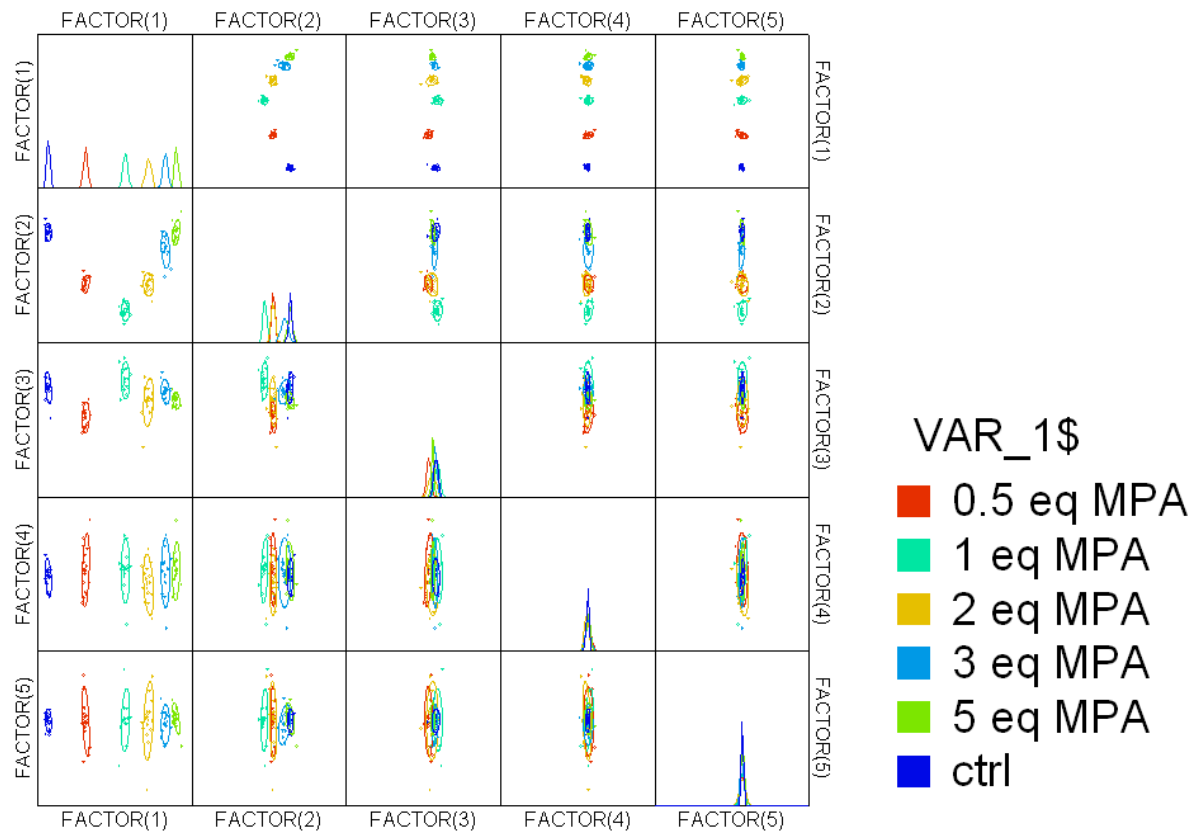


**Figure S32.** LDA canonical scores plots of the quantitative assay of sensor **3** and MPA.

### Jackknifed Classification Matrix

	0.2 eq GlyP	0.4 eq GlyP	1 eq GlyP	2 eq GlyP	4 eq GlyP	6 eq GlyP	ctrl	%correct
0.2 eq GlyP	20	0	0	0	0	0	0	100
0.4 eq GlyP	0	20	0	0	0	0	0	100
1 eq GlyP	0	0	20	0	0	0	0	100
2 eq GlyP	0	0	0	20	0	0	0	100
4 eq GlyP	0	0	0	0	20	0	0	100
6 eq GlyP	0	0	0	0	0	20	0	100
ctrl	0	0	0	0	0	0	20	100
Total	20	20	20	20	20	20	20	100

**Figure S33.** Jackknifed Classification Matrix of the quantitative LDA assay for sensor **3** and GlyP with Pi as an interferent.

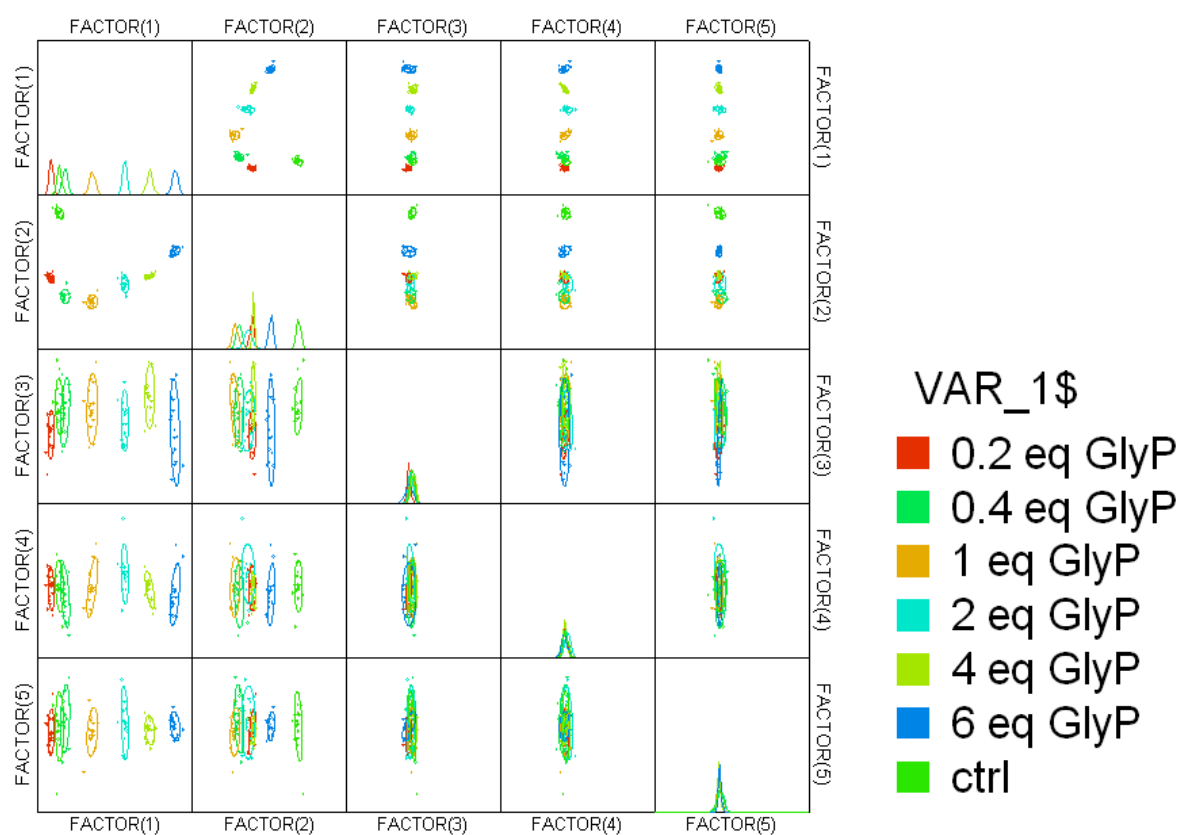


**Figure S34.** LDA canonical scores plot for the quantitative assay for sensor **3** and GlyP with Pi as an interferent.

## Molecular Modeling

Initial geometries of studied molecules were obtained by means of MM computational approach obtained in Avogadro and Monte-Carlo (Maestro). Using Avogadro<sup>3</sup> systematic rotor search was applied (MMFF94), while in the Monte-Carlo conformational sampling

OPLS3e force field (Mixed Torsional/Low-mode sampling - MT/LMOD). In the case of the complex  $\text{H}_2\text{PO}_4^- \subset \mathbf{3}^{2+}$ ,  $\text{H}_2\text{PO}_4^-$  anion was docked in different orientations and subjected to multiple conformational searches. The lowest energy conformer was additionally subjected to the higher level of theory – def2-SVP basis set.<sup>4</sup> All DFT and TD-DFT calculations were performed using Gaussian16<sup>5</sup> package utilizing Ohio Supercomputer Center (OSC)<sup>6</sup> (RMS gradient was below 0.001 kcal/mol). All calculations were conducted in the implicit DMSO solution (dielectric constant = 46.8) utilizing polarizable continuum model (PCM) in the self-consistent reaction field as a method described by Tomasi *et al.*<sup>7,8</sup>

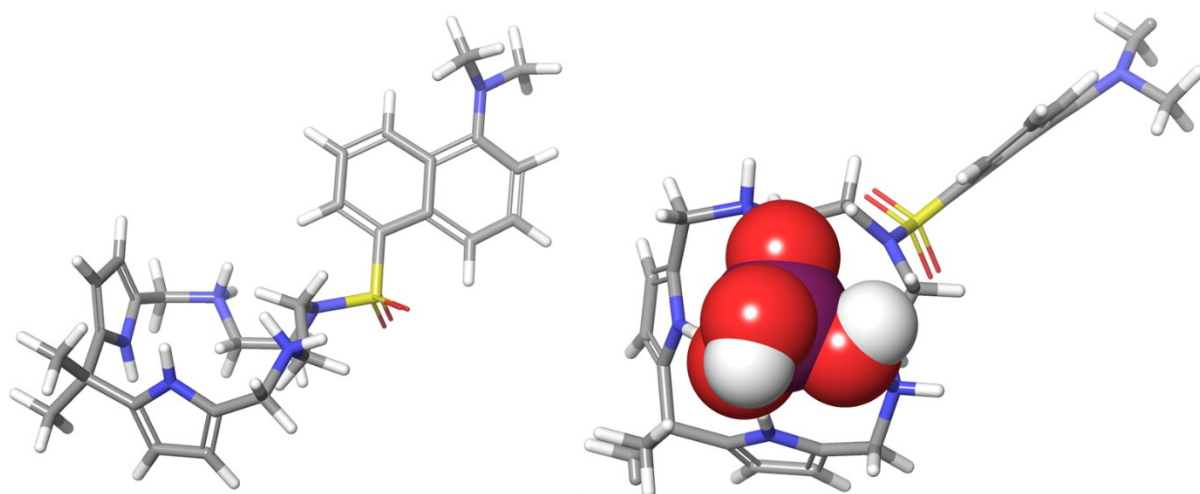


**Figure S35.** Optimized geometries of  $\mathbf{3}^{2+}$ (left), and  $\text{H}_2\text{PO}_4^- \subset \mathbf{3}^{2+}$  (right) in DMSO (PCM) at pbepbe/def2svp level of theory in DMSO (PCM).

Cartesian coordinates (angstroms and degrees) of amine  $\mathbf{3}^{2+}$  in DMSO (PCM) using pbepbe/def2svp level of theory.

2	1			
C		5.12568500	1.71440500	-0.40054000
C		4.50677100	2.67922000	-1.20457900
C		3.44711500	3.25765600	-0.44956400
C		3.43463600	2.63844100	0.80494500
N		4.46583700	1.71123300	0.80654200
C		6.25295600	0.72277900	-0.67830300
C		5.65229700	-0.67140900	-0.52958400
N		4.75251000	-1.16159900	-1.44895100
C		4.22317200	-2.36853400	-1.02003800

C	4.81550200	-2.65930000	0.21338400
C	5.71724400	-1.59963700	0.51735600
C	6.80936500	0.94003200	-2.10242000
C	7.40311800	0.91620000	0.33769100
C	3.19506600	-3.11850300	-1.78027700
C	2.51720100	2.83530800	1.95302500
N	1.30607200	1.87196900	1.94539700
N	1.80837900	-2.42962600	-1.75780400
C	1.20177800	-2.20221700	-0.39651700
C	0.39246800	-0.89138000	-0.39385900
C	1.66858100	0.42256800	2.09809100
C	0.48258500	-0.53593500	2.12072200
N	-0.28615700	-0.58850300	0.86640100
S	-1.86845200	-1.28038100	1.01720200
C	-2.99489600	-0.02606600	0.37512100
O	-1.94079700	-2.45288400	0.10846100
O	-2.11712600	-1.46043700	2.46679000
C	-4.39301200	-0.36859000	0.29979900
C	-5.27722400	0.61627600	-0.28946200
C	-4.75858100	1.90000800	-0.62670700
C	-3.41002800	2.20052300	-0.49126200
C	-2.51195000	1.21650500	-0.01295000
C	-4.94222000	-1.57954500	0.81457800
C	-6.31322900	-1.79416700	0.75549200
C	-7.18159400	-0.87290300	0.12619100
C	-6.68887500	0.30762200	-0.44927200
N	-7.52460300	1.21508900	-1.11521400
C	-7.24435100	1.53627500	-2.51587700

C	-8.94975400	1.17078600	-0.83379700
H	4.79605100	2.93955700	-2.22956200
H	2.76054900	4.05181300	-0.77156400
H	4.71543800	1.10345400	1.59087300
H	4.53120200	-0.69732500	-2.33283800
H	4.61810000	-3.55574800	0.81609100
H	6.34960500	-1.51787900	1.40945900
H	6.02909700	0.83998000	-2.88791000
H	7.61069100	0.20053700	-2.31407600
H	7.24133800	1.95958900	-2.19474600
H	7.06522200	0.80104600	1.38997300
H	7.83233200	1.93503500	0.22937000
H	8.20927600	0.17252300	0.15704100
H	3.04218100	-4.12442000	-1.34598900
H	3.42777000	-3.22626500	-2.86042000
H	2.07219000	3.84850100	1.93329800
H	3.00346800	2.67960400	2.93768900
H	0.65564100	2.15554700	2.70611300
H	1.15859400	-2.98528500	-2.34880600
H	2.04830200	-2.16128100	0.31993400
H	0.55919200	-3.07128300	-0.15838500
H	-0.37900300	-0.92341600	-1.19057900
H	1.06869600	-0.04285600	-0.65196100
H	2.20507400	0.32785800	3.06359000
H	2.38460200	0.18996800	1.28573100
H	-0.22075700	-0.26067400	2.93172100
H	0.90169300	-1.53091200	2.40184300
H	-5.45679400	2.67886100	-0.96731200

H	-3.03258700	3.20406300	-0.74283300
H	-1.44051900	1.44117100	0.07343600
H	-4.29281600	-2.33347000	1.28006000
H	-6.73473600	-2.72211900	1.17628400
H	-8.25104800	-1.11747000	0.05162200
H	-6.16535300	1.43252600	-2.74070800
H	-7.55551200	2.57990700	-2.74652000
H	-7.80292200	0.84916400	-3.20190300
H	-9.12449200	1.09300200	0.25962400
H	-9.47629300	0.32130700	-1.34189500
H	-9.41406500	2.11457900	-1.19484200
H	0.78470300	2.01360900	1.05819600
H	1.90128700	-1.51859800	-2.24926800

Cartesian coordinates (angstroms and degrees) of  $\text{H}_2\text{PO}_4^- \cdot \mathbf{3}^{2+}$  in DMSO (PCM) using pbepbe/def2svp level of theory.

1 1

C	4.80742000	-1.71475100	1.13886200
C	4.39817500	-2.71931600	2.00457400
C	3.56729200	-2.12797400	2.99126000
C	3.49217100	-0.77449900	2.71507900
N	4.26139600	-0.53779500	1.59400900
C	5.64212500	-1.79782200	-0.13477800
C	4.71561400	-1.72539300	-1.34382200
N	4.15007100	-0.54924400	-1.77377200
C	3.29195000	-0.79283100	-2.82578400
C	3.32774500	-2.15128300	-3.08594900
C	4.22832500	-2.73757600	-2.15954300

C	6.69618200	-0.66378700	-0.17862400
C	6.39640400	-3.14244000	-0.15719500
C	2.54900900	0.25704400	-3.56092900
C	2.79948900	0.27581900	3.50191100
N	1.62601000	0.95613300	2.79521600
N	1.46601500	0.97899000	-2.74036600
C	0.68005300	0.12368700	-1.79400600
C	-0.46931000	0.92715200	-1.16049700
C	0.72647100	0.07011300	1.99430400
C	-0.41860000	0.89995400	1.38245100
N	-0.92291100	0.35830300	0.11374400
S	-2.13969600	-0.75633800	0.12447400
C	-3.69415900	0.14108900	0.13724100
O	-2.05257900	-1.48005700	-1.13419100
O	-2.02336600	-1.48080200	1.38018600
C	-4.92439300	-0.59675500	0.12234100
C	-6.14633400	0.15855100	0.09135900
C	-6.08518900	1.57437000	0.16725700
C	-4.88364500	2.24036300	0.20500800
C	-3.67402500	1.51720700	0.16799900
C	-4.99288600	-2.01467600	0.16891900
C	-6.21449800	-2.64460100	0.19292300
C	-7.41850600	-1.91478500	0.11922200
C	-7.41042400	-0.53312300	0.03589500
N	-8.59976000	0.22863900	-0.05869900
C	-8.82564800	0.88079100	-1.35443900
C	-9.81956400	-0.40124800	0.43211500
H	4.66469400	-3.76523300	1.93559300

H	3.08759100	-2.62490900	3.82617800
H	4.33864300	0.36334600	1.11585900
H	4.26673600	0.35620900	-1.31317400
H	2.77657300	-2.65474700	-3.87130700
H	4.48774100	-3.78556500	-2.09553500
H	6.25215200	0.33579700	-0.16450500
H	7.29965500	-0.75058100	-1.09019400
H	7.36635700	-0.74515300	0.68556100
H	5.72040200	-4.00252100	-0.12777600
H	7.06721000	-3.21107900	0.70621700
H	7.00040400	-3.21895400	-1.06798400
H	2.03109800	-0.19974300	-4.40643700
H	3.18415400	1.06538000	-3.93851900
H	3.45576800	1.10322700	3.79379200
H	2.39443400	-0.17661000	4.40945400
H	1.99166900	1.72620600	2.16786300
H	1.90471700	1.75756300	-2.21314400
H	1.38314300	-0.22657500	-1.03841800
H	0.30768700	-0.74177100	-2.34475900
H	-1.30995700	0.98792000	-1.85783200
H	-0.15102600	1.95620000	-0.95930600
H	0.35143400	-0.72600600	2.64070900
H	1.34179800	-0.38497800	1.21834800
H	-0.06777700	1.91691700	1.17654000
H	-1.24076900	0.98640000	2.09846300
H	-7.01373200	2.13282500	0.22227500
H	-4.85476400	3.32456700	0.27198000
H	-2.73516400	2.05993000	0.18177400

H	-4.08649800	-2.60743600	0.20155900
H	-6.25852100	-3.73028400	0.24451100
H	-8.35828100	-2.45720600	0.10237900
H	-7.90523500	1.33061700	-1.73162200
H	-9.57661800	1.67091300	-1.23950400
H	-9.19048400	0.16057900	-2.10864100
H	-9.64966600	-0.82967300	1.42459900
H	-10.20218600	-1.19399000	-0.23585000
H	-10.59740700	0.36632600	0.51490600
O	4.30805300	1.83781800	-0.12258000
O	2.39875400	3.02090600	1.20694600
P	3.41780400	3.02171300	0.10646800
O	2.66609500	3.25223200	-1.33876200
H	5.04713900	4.40657600	-0.28123200
O	4.27484900	4.37753400	0.30371100
H	2.03589800	3.98877300	-1.30201300
H	0.83798400	1.43074300	-3.41077400
H	1.08342800	1.43581600	3.51905300

## References

1. P. Thordarson, *Chem. Soc. Rev.*, 2011, **40**, 1305–1323.
2. Connors, K. A., *The Measurement of Molecular Complex Stability*. **1987**, 432.
3. Hanwell, M. D.; Curtis, D. E.; Lonie, D. C.; Vandermeersch, T.; Zurek, E.; Hutchison, G. R., Avogadro: an advanced semantic chemical editor, visualization, and analysis platform. *J. Cheminformatics*, 2012, **4**, 17.
4. (a) Laikov, D. N., A new class of atomic basis functions for accurate electronic structure calculations of molecules. *Chem. Phys. Lett.*, 2005, **416**, 116-120; (b) Briling, K. R., Comment on "A new parametrizable model of molecular electronic structure", *J. Chem. Phys.*, 2017, **147**, 157101.

5. Frisch, M. J.; Trucks, G. W.; Schlegel, H. B.; Scuseria, G. E.; Robb, M. A.; Cheeseman, J. R.; Scalmani, G.; Barone, V.; Petersson, G. A.; Nakatsuji, H.; Li, X.; Caricato, M.; Marenich, A. V.; Bloino, J.; Janesko, B. G.; Gomperts, R.; Mennucci, B.; Hratchian, H. P.; Ortiz, J. V.; Izmaylov, A. F.; Sonnenberg, J. L.; Williams; Ding, F.; Lipparini, F.; Egidi, F.; Goings, J.; Peng, B.; Petrone, A.; Henderson, T.; Ranasinghe, D.; Zakrzewski, V. G.; Gao, J.; Rega, N.; Zheng, G.; Liang, W.; Hada, M.; Ehara, M.; Toyota, K.; Fukuda, R.; Hasegawa, J.; Ishida, M.; Nakajima, T.; Honda, Y.; Kitao, O.; Nakai, H.; Vreven, T.; Throssell, K.; Montgomery Jr., J. A.; Peralta, J. E.; Ogliaro, F.; Bearpark, M. J.; Heyd, J. J.; Brothers, E. N.; Kudin, K. N.; Staroverov, V. N.; Keith, T. A.; Kobayashi, R.; Normand, J.; Raghavachari, K.; Rendell, A. P.; Burant, J. C.; Iyengar, S. S.; Tomasi, J.; Cossi, M.; Millam, J. M.; Klene, M.; Adamo, C.; Cammi, R.; Ochterski, J. W.; Martin, R. L.; Morokuma, K.; Farkas, O.; Foresman, J. B.; Fox, D. J. *Gaussian 16 Rev. C.01*, Wallingford, CT, 2016.
6. Center., O. S., Ohio Supercomputer Center. **1987**.
7. (a) Tomasi, J.; Mennucci, B.; Cammi, R., Quantum Mechanical Continuum Solvation Models. *Chem. Rev.*, 2005, **105**, 2999-3094; (b) Scalmani, G.; Frisch, M. J., Continuous surface charge polarizable continuum models of solvation. I. General formalism. *J. Chem. Phys.*, 2010, **132**, 114110.
8. (a) Liu, B.; McLean, A. D., Accurate calculation of the attractive interaction of two ground state helium atoms. *J. Chem. Phys.*, 1973, **59**, 4557-4558; (b) van Duijneveldt, F. B.; van Duijneveldt-van de Rijdt, J. G. C. M.; van Lenthe, J. H., State of the Art in Counterpoise Theory. *Chem. Rev.*, 1994, **94**, 1873-1885; (c) Grimme, S.; Antony, J.; Ehrlich, S.; Krieg, H., A consistent and accurate ab initio parametrization of density functional dispersion correction (DFT-D) for the 94 elements H-Pu. *J. Chem. Phys.*, 2010, **132**, 154104; (d) Grimme, S.; Ehrlich, S.; Goerigk, L., Effect of the damping function in dispersion corrected density functional theory. *J. Comp. Chem.*, 2011, **32**, 1456-1465.
9. Vydrov, O. A.; Scuseria, G. E., Assessment of a long-range corrected hybrid functional. *J. Chem. Phys.*, 2006, **125**, 234109.